

## Research Article

# Bioactivity of Citral and Its Nanoparticle in Attenuating Pathogenicity of *Pseudomonas aeruginosa* and Controlling *Drosophila melanogaster*

Aanchal Sharma <sup>1</sup>, Kusum Harjai,<sup>2</sup> Seema Ramniwas <sup>1</sup> and Divya Singh <sup>1</sup>

<sup>1</sup>University Center for Research and Development, Chandigarh University, Mohali 140413, India

<sup>2</sup>Department of Microbiology, Panjab University, Sector 14, Chandigarh 160014, India

Correspondence should be addressed to Seema Ramniwas; [seema.ramniwas@gmail.com](mailto:seema.ramniwas@gmail.com)

Received 18 July 2022; Revised 1 October 2022; Accepted 19 October 2022; Published 23 January 2023

Academic Editor: Dong Kee Yi

Copyright © 2023 Aanchal Sharma et al. This is an open access article distributed under the Creative Commons Attribution License, which permits unrestricted use, distribution, and reproduction in any medium, provided the original work is properly cited.

Plant-based essential oils are hydrophobic, volatile concentrate extracted from aromatic plants. They are the upcoming alternative and appealing source of antimicrobial compounds, citral (major constituent of lemongrass oil) being one of them, whose anti-quorum sensing, in vivo delivery, and insecticidal potential need further exploration. *Pseudomonas aeruginosa* is one of the most prevalent, clinically lethal pathogens, which is resistible toward various treatments because of the inherent resistance acquired by the organism to many classes of drugs (multidrug resistant (MDR)). Moreover, fruit flies have been considered as the vectors of potentially lethal and opportunistic pathogens, including multiantibiotic-resistant microbes. As a result, controlling both the pathogen and its host vector are of utmost importance. The present study focused on the efficacy of essential oil of citral (EOC) and its nanoencapsulated form on quorum sensing inhibition (QSI) of *P. aeruginosa* PAO1 and its insecticidal activity against *Drosophila melanogaster*. Chitosan-based citral nanoparticles were synthesized and characterized using hydrodynamic size, zeta potential, polydispersity index, and field-emission scanning electron microscopy (FE-SEM). Citral nanoparticles at sub-minimum inhibitory concentration (MIC) exhibited QSI potential by attenuating biofilm formation ( $p$ -value < 0.05), while insecticidal activity of citral tested against *D. melanogaster* demonstrated toxicity of the EOC at a concentration of 3%–5%. Hence, the results elucidated the prospects of citral nanoparticles in the delivery of citral, which can be applied as a strategy to specifically target clinically lethal pathogens, major insect pests, and associated microbes.

## 1. Introduction

The present era of antibiotic resistance and sudden emergence of lethal human pathogens are due to the surfacing of multidrug-resistant (MDR) variants worldwide. *Pseudomonas aeruginosa* is one of the intractable pathogens, implicated in a number of lethal nosocomial infections, as the organism is inherently resistant to many classes of drugs, including cephalosporins, aminoglycosides, quinolones, and the carbapenems. Thus, the antibiotic-resistant variants are the main cause of a copious number of clinical infections associated with *P. aeruginosa*. The pathogenesis of the bacterium within the host involves the use of highly sophisticated genotypic events to bolster various molecular and phenotypic mechanisms that

enable it to survive under antibiotic stress [1]. The pathogen achieves clinical irresistibility due to the presence of various virulence factors, which can be extracellular and/or intracellular. In addition to this, *P. aeruginosa* has another outstanding characteristic of forming planktonic and biofilm cells, which enable it to cause both acute and chronic infections. Bacteria create very persistent biofilm cells in tensible conditions, such as those found in cystic fibrosis-infected lungs and viscera, allowing it to live and endure for longer periods of time. Therefore, it is practically impossible to eradicate *P. aeruginosa* infections, which are mediated through the phenomenon of quorum sensing (QS) [2]. Hence, novel strategies need to be implemented that could potentially target the QS of *P. aeruginosa* populations and, hence, could attenuate its

pathogenicity in clinical settings rather than directly killing the pathogen.

The first QS system was elucidated in 1985 and since then, there have been a lot of discussion among researchers about the potential of attenuating the QS system of bacteria in order to restrain its pathogenesis. The quest for reliable QS antagonists has continued ever since, with researchers exploring natural plant-derived products with efficient activity and chemical stability in small doses. This has led to the emergence of new area of research exploration, namely, quorum quenching (QQ), which involves all the means by which QS system of bacteria could be attenuated or hindered. The attenuation of QS system by means of QQ could pay the way for alternate strategy to regulate population density and gene expression and, hence, pathogenesis of bacteria accordingly. The molecular determinants of QQ can be proteinaceous enzymes (QQ enzymes) or chemical analogs (QS inhibitors), which can be competitive/noncompetitive inhibitors of QS signals. Therefore, according to Grandclément et al. [3], “the term QQ encompasses a wide range of complex occurrences and mechanisms.” Moreover, the efficient characterization of QS signaling molecules and their QQ counterparts have revealed that QS inhibitors are significantly more useful than traditional antimicrobials as they put less selection pressure on bacteria by not inducing cell death directly, thereby delaying the onset of antimicrobial resistance. Since time immemorial, many chemicals originating from plants, especially in the form of secondary metabolites, have been employed for their QS inhibiting capability. The antimicrobial activity of these plant-derived compounds is primarily attributed to phytoconstituents such as phenolic compounds, flavonoids, quinones, saponins, tannins, terpenoids, and alkaloids, whose functional and structural organizations are the cause of their QS inhibitory potential. There is a growing consensus that natural plant-derived compounds and their bioactive constituents are exceptionally potent, which can substitute conventional antibiotics. In a recent study, Niaouli essential oil (EO) and its major component 1,8-cineole have been found to be effective against *P. aeruginosa* PAO1 by competitively inhibiting QS [4]. *Lippia origanoides*, *Thymus* spp., and *Satureja hortensis* oil exhibited antibiofilm and QSI activities against human pathogenic bacteria [5, 6]. Furthermore, EOs and their bioactive compounds are eco-friendly and are not liable to bacterial resistance strategies [7]. Citral (a terpenoid), an integral constituent (30%–40%) of essential oil of lemongrass (EOL), is a potent antibacterial, antifungal, palliative, antiparasitic, as well as antianxiety and antidepressant compound whose applicability for curative purposes is rationalized by the fact that the continued vulnerability of its use has not confronted resistance among microorganisms [8, 9]. The full potential of phytoconstituents of EOL remains unexplored, despite their highly efficacious property of QSI at subinhibitory concentration. Researchers have previously shown that plant extracts and their bioactive components (phytochemicals) could efficiently hinder the intra- and interspecific communication system of the microbes, thereby blocking the pathway for microbial pathogenesis inside the host [10–12]. In this context, EO and their phytochemicals

are considered to be safe for human use due to their low molecular mass and chemical stability [13].

The primary focus of the study is on quorum sensing inhibitory (QSI) potential of EO of citral and its polymer-based nanoparticle. Citral belongs to a terpenoid class of phytoconstituents, which is primarily attributed to the antibacterial property of EOL [14]. According to the U.S. Food and Drug Administration (FDA), citral is standardly acclaimed as safe (GRAS 182.10). It is an antibacterial chemical that has been shown to be effective against lethal Gram-positive and Gram-negative bacteria such as *Escherichia coli* strain O157:H7, *Salmonella typhimurium*, *Listeria monocytogenes*, and *Staphylococcus aureus* [15]. Existing literature supports the fact that its effectiveness against *P. aeruginosa* and associated antibacterial activity has yet to be fully demonstrated. Despite being an insoluble hydrophobic compound, citral is completely immiscible in inorganic solvents, incompatible with physiological system, and highly unstable at room temperature. Therefore, its applicability for both in vitro and in vivo purposes would be quite tedious [16, 17]. Encapsulation of citral in the form of nanoparticles, on the other hand, unveiled the much anticipated inhibition of the QS signaling molecules. Various encapsulation procedures have been studied including oil-in-water emulsion, multilayer emulsions, nanohydrogel, polymer encapsulation (such as cyclodextrin-inclusion complexes, polyacrylamide, and alginate polymerization), and self-assembly delivery systems [16–18]. Encapsulation of citral, thus, enhanced the functional potential and antimicrobial property of free oil, which has wide range of applicability from food industry to biomedical and agricultural sector.

Owing to the immense potential of citral, the anti-QS and antibiofilm effects of citral nanoparticles, as well as their characterization, were explored in this article. The secondary focus of the study lies on the insecticidal potential of the EOC. Due to the destruction caused by the insect pests, including fruit fly species against many economically important fruits, it is obligatory to search for alternative strategy in order to target major insect pests and associated microbes with these species. Insecticide resistance has increased as a result of the widespread usage of pesticides making the research focus shifting toward alternative pest management tools, so that potential risks to biodiversity, including nontarget organisms, could be reduced. Moreover, the drosophilids are the well-known carriers/vectors of pathogenic microbes leading to potential risk of infections among humans [19–21]; hence, effective management of these pests requires utmost attention. In the current study, the QSI activity of citral and its nanoparticle (polymer-based) against *P. aeruginosa* PAO1 have been investigated. Moreover, the toxic effect of citral against *Drosophila melanogaster* demonstrated insecticidal potential of citral, which can be further exploited against other pest species in India.

## 2. Materials and Methods

**2.1. Maintenance of Bacterial Strains.** Two biosensor strains, namely, *Agrobacterium tumefaciens* NLT4 and *E. coli* MG4

(both obtained from Jo Handelsman, University of Wisconsin, USA), were used in the present study, which were incubated at 28°C and 37°C, respectively, overnight under static conditions. Two laboratory isolates *E. coli* and *S. aureus* and standard strain of *P. aeruginosa* PAO1 (MTCC-3541, obtained from BH Iglwesi, Department of Microbiology and Immunology, University of Rochester, USA) were cultured in Luria Broth (LB) at 37°C overnight (150 rpm).

**2.2. *Drosophila melanogaster* Collection and Rearing.** Wild caught Canton-S flies (*D. melanogaster*) were collected for experimental purpose from Kharar, Punjab (latitude and longitude coordinates: 30.751278 and 76.637192). Flies were grown under laboratory conditions (25 ± 1°C and 60%–70% relative humidity) by rearing on standard *Drosophila* medium, which consists of the predetermined fractions of various components such as agar–agar (15 g), dry yeast powder (40 g), sugar (64 g), and corn meal powder (72 g) per liter of water. Sodium benzoate (3 g) and propionic acid (6 ml) were also added as antimicrobial agents.

**2.3. Estimation of Minimum Inhibitory Concentration (MIC) of Citral.** Minimum inhibitory concentration (MIC) of citral required to inhibit the growth of *P. aeruginosa* PAO1 was evaluated by colorimetric method using resazurin microtiter assay (REMA) as described by Drummond and Waigh [22]. Briefly, stock solution of citral was serially diluted from 40% to 5% (in 10% dimethyl sulfoxide (DMSO)), followed by incubation at 37°C for 18 hr. After the addition of 10 µl of 0.01% resazurin dye (incubated for 1 hr), the maximum dilution showing no color change (from blue to pink) was considered as the MIC of citral.

**2.4. Evaluation of Quorum Sensing Inhibitory (QSI) Activity of Citral.** The estimation of QSI activity of citral was performed by the method of Shaw et al. [23] in which acyl homoserine lactone (AHL) was extracted by inoculating *P. aeruginosa* PAO1 in LB at 37°C (overnight) under continuous shaking conditions (150 rpm). The resulting culture was then centrifuged at 10,000 rpm for 15 min and the supernatant collected was pooled. AHL was extracted by centrifugation at 10,000 rpm for 15 min and the supernatant was dissolved in acidified ethyl acetate (0.01%) at 4°C (overnight). The organic layer was separated and the ethyl acetate was removed using Rotavapor resulting in 1 ml of AHL solution in the supernatant. The solution was stored at 4°C for further use. About 100 µl of extracted AHL was spread on a petri plate with initially streaked overnight culture of *A. tumefaciens* NLT4 and *E. coli* MG4 in separate plates. The petri plates were kept undisturbed at room temperature (RT) for 10 min. About 30 µl of citral (50%, 25%, 20%, and 15% in 5% DMSO) was loaded in 5 mm diameter wells punched on the plates. Negative control well contained 5% DMSO. Incubation at 28°C (*A. tumefaciens* streaked plates) and 30°C (*E. coli* MG4 streaked plates) for overnight was given and observed for degradation of AHL (colorless zones) on the next day.

**2.5. Synthesis of Chitosan-Based Nanoparticles.** Polymeric-based citral nanoparticles were synthesized by the method

of Anitha et al. [24] in which chitosan sulfate (CS) and tripolyphosphate (TPP) (Sigma-Aldrich Chemical Co. Ltd., St. Louis, USA) were combined in different ratios (1 : 1, 1 : 2, 3 : 1 (CS:TPP) (v/v)). Briefly, citral (6% in methanol) was loaded to CS (1% acetic acid) solution dropwise followed by TPP (in high-performance liquid chromatography (HPLC) grade water) by continuous magnetic stirring for 1 hr. Residual methanol was evaporated using Rotavapor. Opalescent formulation was chosen for further experimentation.

**2.5.1. Characterization of Nanoparticles.** Citral nanoparticles were characterized by following parameters: particle size, zeta potential, polydispersity index (PDI), field-emission scanning electron microscopy (FE-SEM), entrapment efficiency (%EE), and in vitro release kinetics. Particle size and PDI were analyzed by Zetasizer Nano ZS (Malvern Instruments, UK) at 25°C [25]. Malvern Instruments Dispersion Technology software (version 4.0) was used to control and analyze all data from the instrument [26]. FE-SEM was performed using Joel Ion Sputter (JFC-1100) at Sophisticated Analytical Instrumentation Facility (SAIF), Panjab University, Chandigarh. The samples were examined by using FE-SEM model S-4160 (Hitachi, Japan). The %EE of citral within the CS-TPP nanoparticles and in vitro release profile was determined by the method of Sharma et al. [27]. The in vitro release profile of citral from nanoparticles was carried in order to understand the release behavior of citral from nanoparticles for sustained release of citral in vivo. The study was carried out at two different pH (5 and 7.4) using acetate buffer and phosphate-buffered saline (PBS), respectively, as release medium to mimic the in vivo conditions. The %EE was calculated using the following formula:

$$\%EE = \frac{\text{Total amount of loaded essential oils}}{\text{Initial amount of loaded essential oils}} \times 100. \quad (1)$$

**2.6. Estimation of Minimum Inhibitory Concentration (MIC) of Citral Nanoparticles.** MIC of citral nanoparticles was determined by the method of Jadhav et al. [28] with slight modifications. Briefly, citral nanoparticles (100, 90, 80, 70, 60, and 50 µl) were added to 5 ml of LB tubes separately, followed by 50 µl of OD (absorbance at 600 nm = 0.3) set culture of *P. aeruginosa* PAO1. Positive control tube contained only 50 µl OD set culture, while negative control tube contained uninoculated media. After overnight incubation at 37°C under shaking conditions, tubes were then observed for visible growth. The results were interpreted as the maximum dilution, which showed that no visible growth in tubes was chosen as MIC of citral nanoparticles. The experiment was performed in triplicates.

**2.7. Estimation of Sub-Minimum Inhibitory Concentration (Sub-MIC) of Citral Nanoparticles.** Sub-MIC was determined using growth curve analysis to measure a concentration at which the citral nanoparticles could attenuate the virulence of *P. aeruginosa* without killing it. Briefly, citral nanoparticles (100, 90, 80, 70, 60 µl/ml) were added to 20 ml of LB. 200 µl

of OD 600 set culture (0.3–0.4) of *P. aeruginosa* PAO1 was added to each tube. A blank flask contained the respective volume of bare nanoparticles, while a positive control flask contained 200  $\mu\text{l}$  of culture only. Incubation at 37°C under shaking conditions (150 rpm) was given and an aliquot was withdrawn at different time intervals: 0, 2, 4, 6, 8, 10, 12, and 24 hr for measuring the absorbance at 595 nm. The blank absorbance value was subtracted from the respective absorbance values of flasks containing citral nanoparticles. Growth curve (OD (at 595 nm) vs. time (in hours)) was plotted using Microsoft Excel. The sub-MIC was chosen as that concentration of citral nanoparticles when it does not have an effect on growth of *P. aeruginosa*.

**2.8. Qualitative Estimation of QSI Activity of Citral Nanoparticles.** QSI activity of citral nanoparticles and citral (alone) was performed using agar well diffusion assay. AHL was extracted from *P. aeruginosa* PAO1 as described earlier. Wells were loaded with 30  $\mu\text{l}$  of citral, citral nanoparticles (90, 80, 70, 60  $\mu\text{l}/\text{ml}$ ), and bare nanoparticles. The plates were incubated at 28°C overnight and observed for degradation of AHL (colorless zones) on the next day. The inhibition zones around the wells corresponded to the bactericidal activity, while the colorless zones of colonies represented the anti-QS potential of the agent.

### 2.9. Evaluation of Antibiofilm Activity of Citral Nanoparticles

**2.9.1. Biofilm Inhibition Assay.** Biofilm formation and the inhibition effect due to citral nanoparticles were performed according to the method of Stepanović et al. [29]. Briefly, 100  $\mu\text{l}$  of overnight grown *P. aeruginosa* PAO1 was added to each well of 96-well microtiter plate. Negative control well contained 200  $\mu\text{l}$  of LB, while the treatment wells contained citral nanoparticles (90, 80, 70, 60  $\mu\text{l}/\text{ml}$ ) and citral (2  $\mu\text{l}/\text{ml}$ ), separately along with 100  $\mu\text{l}$  of LB to equilibrate the volume. To allow biofilm formation, incubation at 37°C (overnight) under static conditions was given and after 18–24 hr, spent media was replaced by fresh media (to eliminate planktonic cells) by washing thrice with 0.1 M sterile PBS (pH 7.2). The inner surface of the wells was scrapped using a sterile scalpel blade, and then, the cells were suspended in 100  $\mu\text{l}$  of PBS (pH 7.2). Everyday, the suspended cells in PBS were serially diluted and 25  $\mu\text{l}$  of each dilution was plated on MacConkey agar plates (incubation at 37°C for 18 hr). The log bacterial count (log<sub>10</sub> colony-forming unit (CFU)/ml) was determined consecutively for 7 days.

**2.9.2. Microscopic Analysis (FE-SEM).** Microscopic visualization of treated and untreated biofilm cells was done using FE-SEM. Treated biofilm cells were formed in the presence of sub-MIC of citral nanoparticles and citral over acid-etched coverslips for 48 hr. Coverslips were then fixed using 2.5% glutaraldehyde in 0.1 mM PBS for 6–12 hr at 22°C, followed by washing with 0.1 M sterile PBS (pH 7.2) and dehydration with increasing concentrations of ethanol (50%–100%) at RT. Samples analysis was done using Joel Ion Sputter (JFC-1100) at SAIF, Panjab University, Chandigarh.

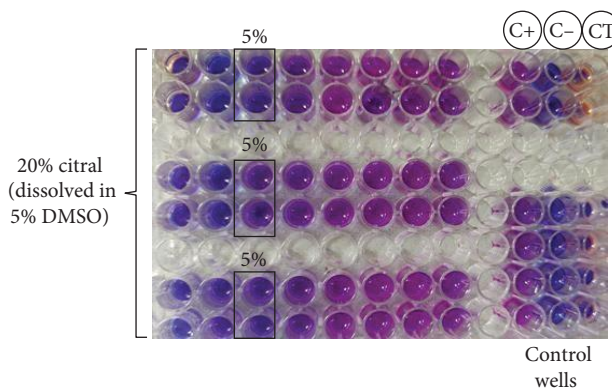


FIGURE 1: A 96-well microtiter plate showing MIC of citral against *P. aeruginosa* PAO1. (C+): positive control well; (C-): negative control well; (CT): citral control well.

**2.10. Insecticidal Activity of Citral against *Drosophila melanogaster*.** Insecticidal potential of citral was determined against *D. melanogaster* for the following citral concentrations: 0.5%, 0.2%, 1%, 3%, and 5%. Briefly, 20 females and 20 males (6 days old) of *D. melanogaster* were kept on standard *Drosophila* culture medium for 6–8 hr of egg laying. Around 30 eggs were counted and placed in each petri plate containing varying concentrations of citral, followed by incubation into a biochemical oxygen demand incubator at 25°C. The assay measured following attributes: %adult emergence, %survivability, and development time. Negative control consisted of 0.1% Tween 80 supplemented in *Drosophila* culture medium without citral.

**2.11. Statistical Analysis.** Microsoft Excel 2010 was used for statistical analysis of the data. The experiments were performed in triplicates, which were represented as the average of standard deviation. Tests performed were Student's *t*-test, one-way and two-way ANOVA, which analyzed the differences between control and test treatments. Data with *p*-value < 0.05 were considered statistically significant.

## 3. Results and Discussion

**3.1. Minimum Inhibitory Concentration of Citral.** MIC of citral was determined by resazurin dye reduction assay in which color change using resazurin dye (from blue to pink) is the indicator of cell viability. Citral (20% v/v in 5% DMSO) was serially diluted in 96-well microtiter plates. Negative control well consisted of media without inoculum (no viable cells), while the positive control well consisted of culture media (indicator of viable bacterial cells). MIC of citral required to inhibit *P. aeruginosa* growth was around 5% (v/v), as determined by the assay (Figure 1). The results were concurrent with previous findings of Hayes and Markovic [30], Aiensaard et al. [31], and Adukwu et al. [14], where it was claimed that citral is effective in inhibiting the growth of pathogenic bacteria of clinical significance. According to Gill et al. [32], antibacterial potential of EO could be primarily due to the individual components of the oil, acting synergistically for more potent effect.

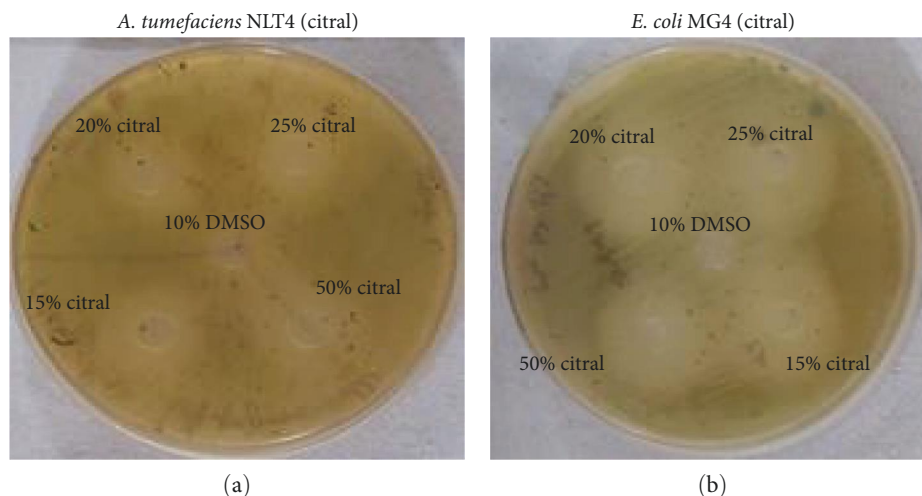


FIGURE 2: Plates showing QSI activity of citral against: (a) *A. tumefaciens* NLT4; (b) *E. coli* MG4.

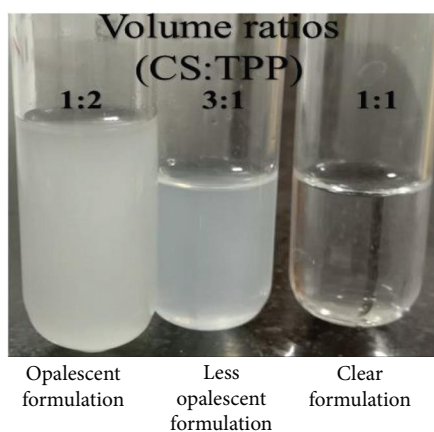


FIGURE 3: Chitosan-tripolyphosphate (CS-TPP)-based citral nanoparticles.

**3.2. Quorum-Sensing Inhibitory (QSI) Activity of Citral.** QSI activity of citral was determined using biosensor strains: *A. tumefaciens* NLT4 and *E. coli* MG4; the nonpigmented colonies around the wells are the indicator of QSI activity, while complete inhibition of growth represented the antibacterial activity of citral. These colorless colonies formed around the wells qualitatively represented the attenuation of virulence or QS potential of the citral. Control well contained 10% DMSO in sterile distilled water. As shown in Figure 2, all concentrations of citral exhibited antibacterial and QSI activity but at 20% and 25%, prominent anti-QS activity can be clearly observed. At 20% and 25% of pure citral, colorless colonies were formed at vicinity of inhibitory zone around the well. In contrast, 15% of citral showed weak antibacterial activity, while 50% of oil showed clear inhibitory zone around the well.

**3.3. Synthesis of Citral Nanoparticles.** CS- and TPP-based citral nanoparticles were prepared for the encapsulation of oil in order to curb the problem of solubility and delivery of EO of citral. As shown in Figure 3, volume ratio of 1 : 2

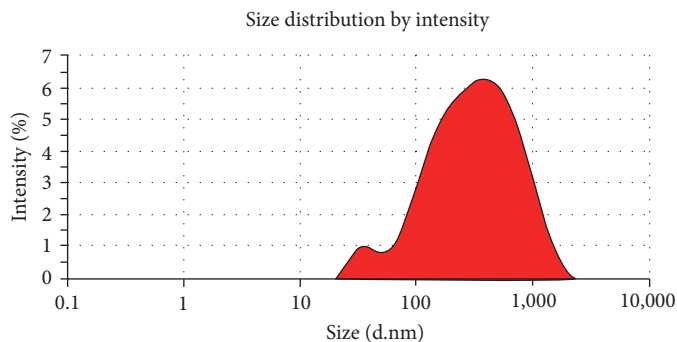
(CS:TPP) formed opalescent formulation without the aggregate formation. Hence, this volume ratio was used for further experiments. Loading of citral in the form of polymeric nanoparticles showed that citral completely got soluble when emulsified in CS-TPP nanoparticle formulation. This formulation combated the problem for delivery of citral for in vivo applications.

**3.3.1. Characterization of Citral Nanoparticles.** Characterization of citral nanoparticles was done by Zetasizer where average hydrodynamic size and PDI were found to be  $209 \pm 22.4$  nm and 0.490, respectively, as shown in Figure 4(a). These results verified that citral nanoparticles were relatively uniform or homogeneously distributed within the colloidal system in accordance with the particle size. The results of zeta potential (surface charge indicator), as shown in Figure 4(b), elucidated that the potential difference between the nanoparticle and its dispersion medium was  $20.9 \pm 3.54$  mV. Both zeta potential and PDI are the parameters of stable nanoformulation formation. Moreover, FE-SEM analysis was performed to visualize the topological details (size and shape) of formed citral nanoparticles, which displayed typically spherical shape of nanoparticles, as shown in Figure 4(c). While the shape of nanoparticle could influence its delivery have been the topic of research among the scholars, the significance of a particular shape of nanomaterial is still to be delineated. Hence, a particular shape of nanosized materials can indispensably affect its transportation and absorption within the human body, regardless of the specific routes of administration. A study done by Chenthamara et al. [33] claimed that, “the spherical nanoparticles transverse freely due to their basic symmetry, while the nonspherical particles thrust or sink within the dispersion medium.” The in vitro release profile revealed that there was an initial fast release till the first 6 hr where citral was released up to 46% in pH 5 (sodium acetate buffer) and 38% in pH 7.4 (PBS). The release rate slowed down after 24 hr, but sustained release was observed till 144 hr. Drug release was up to 80% and 78% at pH 5 and

## Results

	Size (d.nm)	%intensity	Standard deviation (d.nm)	
Z-average (d.nm) 209.9	Peak 1	421.2	95.1	329.8
PDI 0.490	Peak 2	37.06	4.9	8.490
Intercept 0.881	Peak 3	0.000	0.0	0.000

Result quality **Good**



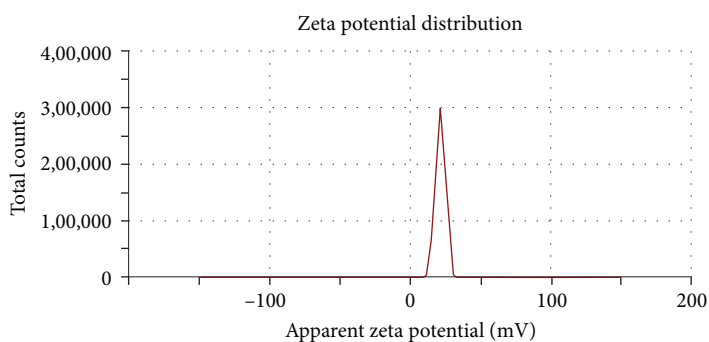
■ Record 52: A-NPs 1

(a)

## Results

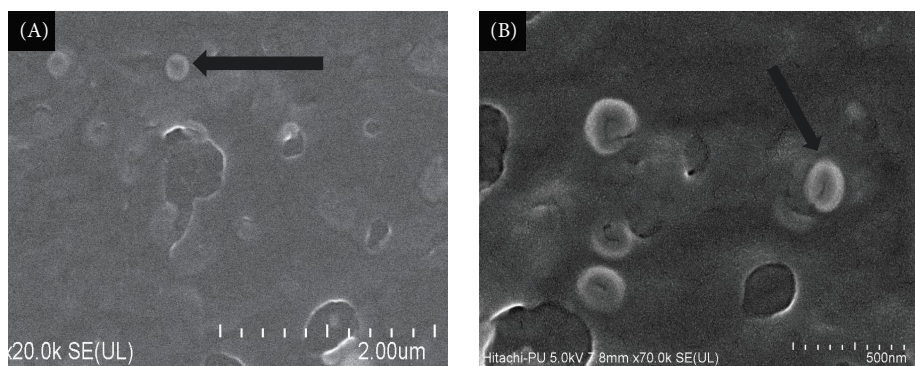
	Mean (mV)	Area (%)	Standard deviation	
Zeta potential (mV) 20.9	Peak 1	20.9	100.0	3.54
Zeta deviation (mV) 3.54	Peak 2	0.00	0.0	0.00
Conductivity (mS/cm) 0.836	Peak 3	0.00	0.0	0.00

Result quality **Good**



— Record 381: A-NPs 1

(b)



(A) Citral-loaded chitosan nanoparticles

(B) Citral-loaded chitosan nanoparticles

(c)

FIGURE 4: Continued.

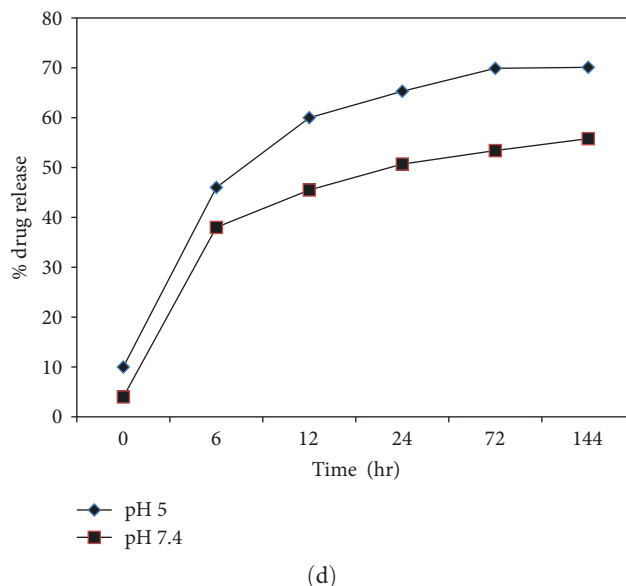


FIGURE 4: (a) Data sheet representing the  $z$ -average (particle size), polydispersity index (PDI), and quality check of citral nanoparticles. (b) Data sheet representing zeta potential (mV) and result quality of citral nanoparticles. (c) (A and B) FE-SEM images of citral nanoparticles. Arrows in the image denote formed nanoparticles. (d) In vitro release profile of citral from nanoparticles at neutral (7.4) and acidic (5) pH.

pH 7.4, respectively (Figure 4(d)). These results were concurrent with previous study, which indicated a time- and pH-dependent in vitro release of EO into release media with a rapid initial release of EO and a steady state phase of EO at the later stages [34]. The %EE of citral oil was found to be around  $52.56\% \pm 4.89\%$ . These results are similar to those in the former investigation, except for results of microencapsulation efficiency of lemongrass oil using spray drying where %EE was  $84.75\%$  [35]. However, %EE of lemongrass oil encapsulated in CS nanoparticles was  $44.82\% \pm 2.80\%$  as investigated by Negi and Kesari [36].

**3.4. Minimum Inhibitory Concentration (MIC) of Citral Nanoparticles.** For the estimation of MIC, macrodilution tube method was performed in order to elucidate the minimum concentration of citral nanoparticles required to inhibit the growth of *P. aeruginosa* PAO1. Estimated MIC of citral nanoparticles was observed to be  $100\mu\text{l/ml}$  relative to the negative control with no visible growth, as shown in Figure 5.

**3.5. Sub-MIC of Citral Nanoparticles.** In order to determine the subinhibitory concentration of citral nanoparticles, growth profile of standard strain of *P. aeruginosa* was created by growing the bacterium in the presence and absence of citral nanoparticles below the MIC. According to the definition, sub-MIC is that concentration of the drug/agent at which virulence or pathogenicity of the strain is suppressed instead of doses, which can directly kill the microorganism. Growth profile of *P. aeruginosa* observed over a period of 10 hr demonstrated that the lag phase (initial hours from 0 to 2 hr) showed no significant alteration in the growth of *P. aeruginosa*. However, during exponential phase (4–10 hr), a relatively similar growth profile was observed with citral nanoparticles at  $80\mu\text{l/ml}$  and the control (without treatment). Hence, growth kinetics showed that this volume of citral

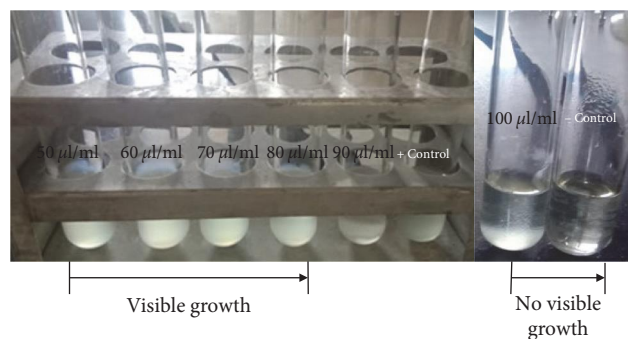


FIGURE 5: Macro-dilution tube method representing MIC of citral nanoparticles. –Control: negative control tube (only LB); +control: positive control tube (culture media without treatment).

nanoparticles did not significantly inhibit the growth of *P. aeruginosa* and this value was further deployed in vitro experiments of QSI activity. In contrast, a considerable inhibition of growth was observed at 100 and  $90\mu\text{l/ml}$  of citral nanoparticle, as shown in Figure 6.

**3.6. QSI Activity of Citral Nanoparticles.** Biosensor strain, *A. tumefaciens* NLT4, was used to determine the potential of citral nanoparticles to inhibit long-chain AHLs in a concentration-dependent manner. A colorless zone of colonies around the wells was observed at sub-MIC ( $80\mu\text{l}$ ) and below MIC ( $60, 70, 90\mu\text{l/ml}$ ) of citral nanoparticles, which clearly indicated the QSI activity. Antibacterial activity was more evident at higher concentration ( $90\mu\text{l/ml}$ ) of citral nanoparticles than QSI activity, as shown in Figures 7(a) and 7(b), whereas lower concentrations ( $60$  and  $70\mu\text{l/ml}$ ) showed minimal to no QSI activity, as shown in Figure 7(c). Moreover, encapsulated citral showed better QSI activity than citral alone. This is the first data reporting the QSI

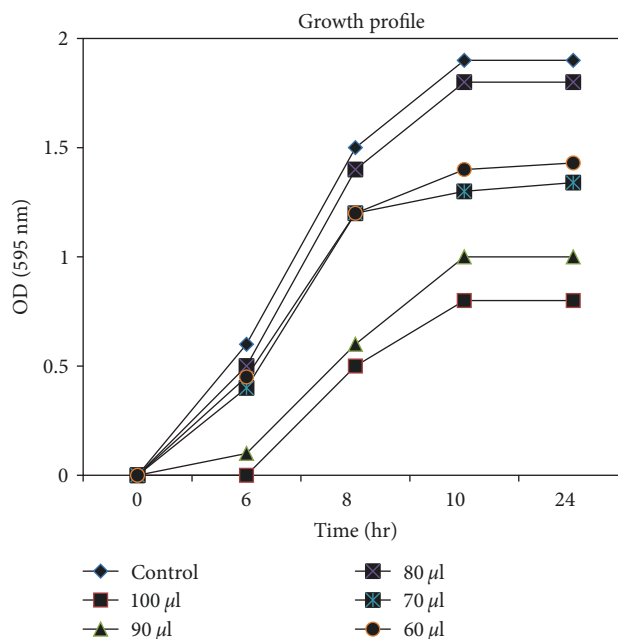


FIGURE 6: Growth kinetics of *P. aeruginosa* PAO1 with and without citral nanoparticle treatment.

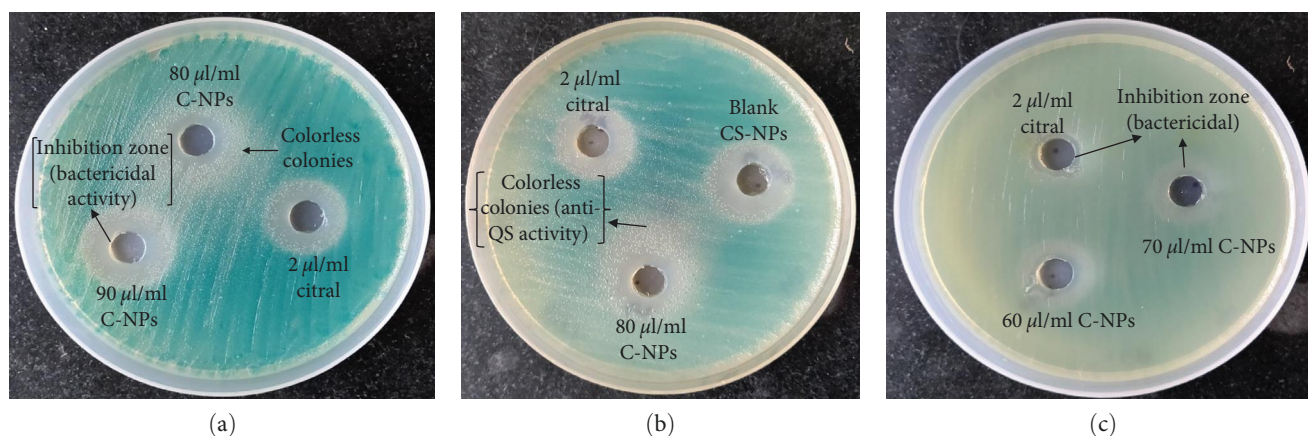


FIGURE 7: Quorum sensing inhibitory (QSI) activities of (a) 80  $\mu$ l/ml of citral nanoparticles (C-NPs) and 90  $\mu$ l/ml of citral nanoparticles, (b) blank chitosan nanoparticles (CS-NPs) and 80  $\mu$ l/ml nanoparticles, and (c) 60 and 70  $\mu$ l/ml of citral nanoparticles, compared with citral alone.

activity of citral nanoparticles, which can be further used for biomedical applications.

From the results of above experiments, it can be concluded that the antimicrobial and QSI effects of citral nanoparticles are more potent than the free form of citral. These findings are coherent with similar study with cinnamon (*Cinnamomum zeylanicum*), thyme (*Thymus vulgaris*), clove (*Syzygium aromaticum*), and *Schinus molle* EO when encapsulated with the CS nanoparticles and showed enhanced antimicrobial activity than the CS and EOs alone [37–39]. However, not a single article reports QSI activity of nanoparticles/EOs in comparison with their free EO. The results support the fact that the nanoparticles could prove to be an effective agent in controlling lethal microbial infections, possibly due to the synergistic effect of CS-TPP-based nanoparticles. However, there are various drawbacks and implications associated with the construction of suitable drug

delivery systems such as carrier for the targeted drug delivery and physical and chemical factors, which are pivotal for the bioavailability of drug and could offer potential pathway to combat several identified target diseases.

**3.7. Effect of Citral Nanoparticles on Biofilm Phenotypes.** The effect of citral nanoparticles was phenotypically observed on biofilm-forming ability of *P. aeruginosa* for up to 7 days. The results (Figure 8(a)) clearly depicted that biofilm-forming capacity of the bacterium retarded in the presence of citral nanoparticles at all concentrations. However, at sub-MIC, significant inhibition of about 3.2 log and 2.0 log was observed on 6th and 7th days ( $p$ -value < 0.05) in comparison with the untreated control. Relative to citral alone-treated biofilm cells, at a very low concentration of 80  $\mu$ l/ml, citral nanoparticles showed antibiofilm activity, which is quite suitable for in vivo purposes with no to less toxicity for clinical patients.



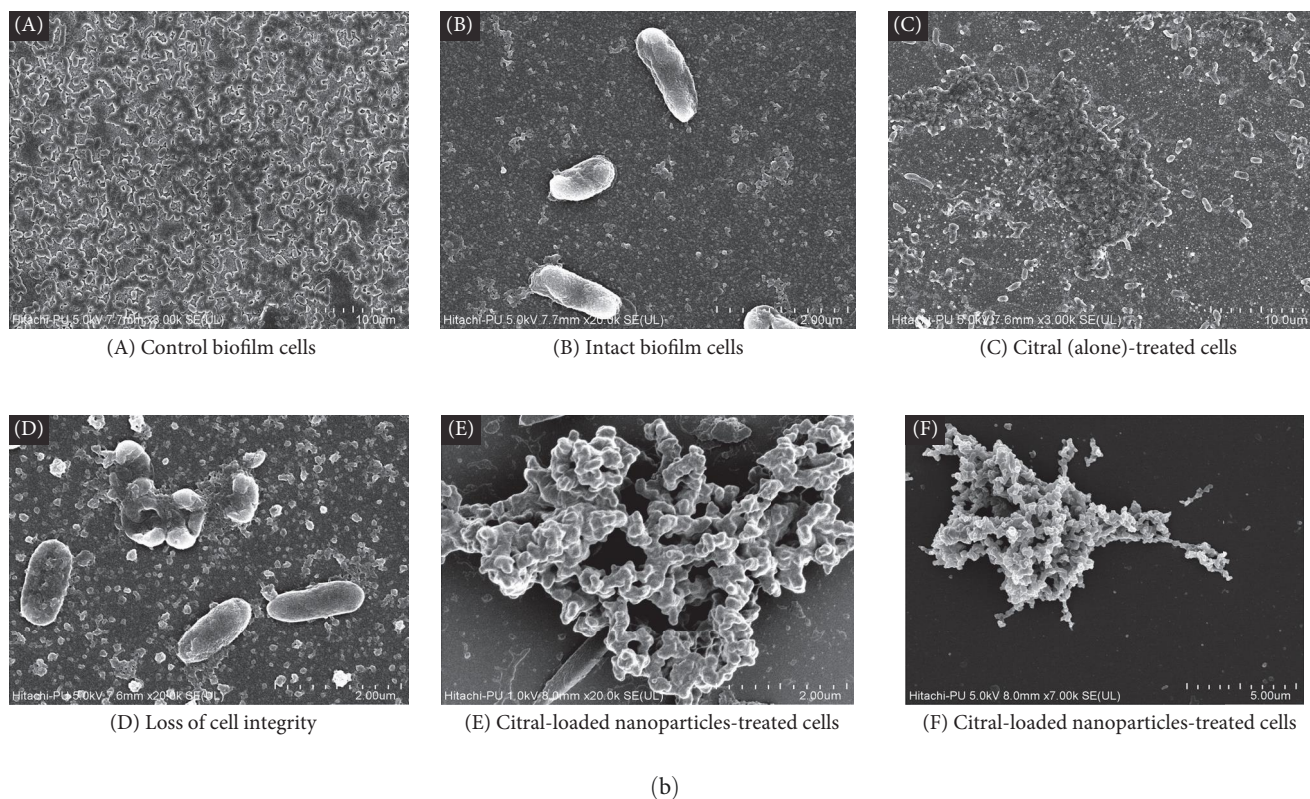
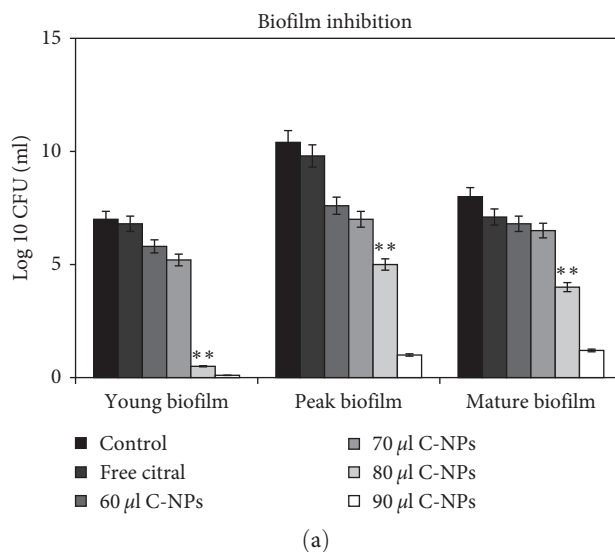


FIGURE 8: (a) Bacterial load of biofilm cells grown for 7 days treated with citral nanoparticles and citral (alone). (b) FE-SEM analysis of: (A and B) control biofilm cells; (C and D) citral (2  $\mu$ l/ml) alone; (E and F) citral nanoparticles (80  $\mu$ l/ml) treated biofilm cells.

Antibiofilm effect of citral nanoparticles was also confirmed by FE-SEM analysis. 48 hr biofilm cells of *P. aeruginosa* were grown in the absence (control) and presence of sub-MIC of citral nanoparticles over acid-etched coverslips under static conditions. The treated cells showed a drastic reduction in biofilm thickness. The entire structure of biofilm cells (amorphous) was skewed when treated with at sub-MIC of citral nanoparticles relative to citral treatment, where insignificant deformation was observed, as shown in Figures 8(B) and 8(D).

Thus, FE-SEM analysis of biofilms validated the fact that the citral nanoparticles (Figure 8(B)–8(D)) are efficient in imparting cell distortion and impaired architecture to biofilm cells at subinhibitory conditions.

3.8. Toxic Effect of Essential Oil of Citral at Different Concentrations against *Drosophila melanogaster*. Insecticidal potential of EO of citral was also monitored against *D. melanogaster* in terms of elongation in developmental

TABLE 1: Toxic effect of essential oil of citral at different concentrations on the developmental stages of *Drosophila melanogaster*.

Treatments (%)	Development time (average)		Adult hatchability (%)	Survivability (%)
	Third instar larvae (days)	Pupa (hr)		
0 (negative control)	4	48	81.4	44
0.2	6	50	78.9	30
0.5	6	39	78.9	34
1	5.5	49	76.1	36
3	11	72	Unfinished	0
5	Unfinished	Unfinished	Unfinished	0

period, % adult hatchability, and % survivability of egg. All obtained results are summarized in Table 1.

#### 4. Conclusion

Results of the present study elucidated that citral nanoparticles could effectively suppress the pathogenicity of *P. aeruginosa* and as a result, it can be utilized for the targeted delivery of citral to treat lethal infections. This property of citral nanoparticles can be used for drug targeting, which can be exploited in treating bacterial complications in clinical settings, including *P. aeruginosa*. Moreover, the elucidation of insecticidal activity of citral against *D. melanogaster* could further be exploited in controlling pests of agricultural importance and associated opportunistic microbes with these pest species of fruit fly. The results of the present study clearly depicted that encapsulation of citral in the form of nanoparticles enhanced the potential of citral in targeted delivery of drug in vivo and, hence, could be used as a potent substitute to conventional antibiotics and chemical insecticides, combating the major problem of antibiotic and insecticide resistance in nature.

#### Data Availability

The data used to support the findings of this study are included within the article. Further data or information is available from the corresponding author upon request.

#### Conflicts of Interest

The authors declare that they have no conflicts of interest.

#### Funding

This work was supported by Panjab University, Sector 14, Chandigarh, and Chandigarh University, Gharuan, Punjab, India.

#### References

- [1] M. F. Moradali, S. Ghods, and B. H. A. Rehm, "Pseudomonas aeruginosa lifestyle: a paradigm for adaptation, survival, and persistence," *Frontiers in Cellular and Infection Microbiology*, vol. 7, Article ID 39, 2017.
- [2] A. Tahrioui, R. Duchesne, E. Bouffartigues et al., "Extracellular DNA release, quorum sensing, and PrrF1/F2 small RNAs are key players in *Pseudomonas aeruginosa* tobramycin-enhanced biofilm formation," *npj Biofilms and Microbiomes*, vol. 5, no. 1, Article ID 15, 2019.
- [3] C. Grandclément, M. Tannières, S. Moréra, Y. Dessaux, and D. Faure, "Quorum quenching: role in nature and applied developments," *FEMS Microbiology Reviews*, vol. 40, no. 1, pp. 86–116, 2016.
- [4] E. Onem, A. Soyocak, M. T. Muhammed, and A. Ak, "In vitro and in silico assessment of the potential of niaouli essential oil as a quorum sensing inhibitor of biofilm formation and its effects on fibroblast cell viability," *Brazilian Archives of Biology and Technology*, vol. 64, Article ID e21200782, 2021.
- [5] M. Cáceres, W. Hidalgo, E. Stashenko, R. Torres, and C. Ortiz, "Essential oils of aromatic plants with antibacterial, anti-biofilm and anti-quorum sensing activities against pathogenic bacteria," *Antibiotics*, vol. 9, no. 4, Article ID 147, 2020.
- [6] A. Sharifi, A. Mohammadzadeh, T. Zahraei Salehi, and P. Mahmoodi, "Antibacterial, antibiofilm and anti-quorum sensing effects of *Thymus daenensis* and *Satureja hortensis* essential oils against *Staphylococcus aureus* isolates," *Journal of Applied Microbiology*, vol. 124, no. 2, pp. 379–388, 2018.
- [7] A. Borges, A. C. Abreu, C. Dias, M. J. Saavedra, F. Borges, and M. Simões, "New perspectives on the use of phytochemicals as an emergent strategy to control bacterial infections including biofilms," *Molecules*, vol. 21, no. 7, Article ID 877, 2016.
- [8] P. Hersch-Martínez, B. E. Leños-Miranda, and F. Solórzano-Santos, "Antibacterial effects of commercial essential oils over locally prevalent pathogenic strains in Mexico," *Fitoterapia*, vol. 76, no. 5, pp. 453–457, 2005.
- [9] H. B. Martins, N. das Neves Selis, C. L. Silva e Souza et al., "Anti-inflammatory activity of the essential oil citral in experimental infection with *Staphylococcus aureus* in a model air pouch," *Evidence-Based Complementary and Alternative Medicine*, vol. 2017, Article ID 2505610, 10 pages, 2017.
- [10] D. A. Vattem, K. Mihalik, S. H. Crixell, and R. J. C. McLean, "Dietary phytochemicals as quorum sensing inhibitors," *Fitoterapia*, vol. 78, no. 4, pp. 302–310, 2007.
- [11] A. J. Bai and R. R. Vittal, "Quorum sensing inhibitory and anti-biofilm activity of essential oils and their *in vivo* efficacy in food systems," *Food Biotechnology*, vol. 28, no. 3, pp. 269–292, 2014.
- [12] R. Barbieri, E. Coppo, A. Marchese et al., "Phytochemicals for human disease: an update on plant-derived compounds antibacterial activity," *Microbiological Research*, vol. 196, pp. 44–68, 2017.
- [13] H. Tang, G. Porras, M. M. Brown et al., "Triterpenoid acids isolated from *Schinus terebinthifolia* fruits reduce *Staphylococcus aureus* virulence and abate dermonecrosis," *Scientific Reports*, vol. 10, no. 1, Article ID 8046, 2020.

- [14] E. C. Adukwu, S. C. H. Allen, and C. A. Phillips, "The anti-biofilm activity of lemongrass (*Cymbopogon flexuosus*) and grapefruit (*Citrus paradisi*) essential oils against five strains of *Staphylococcus aureus*," *Journal of Applied Microbiology*, vol. 113, no. 5, pp. 1217–1227, 2012.
- [15] C. Shi, K. Song, X. Zhang et al., "Antimicrobial activity and possible mechanism of action of citral against *Cronobacter sakazakii*," *PLOS ONE*, vol. 11, no. 7, Article ID e0159006, 2016.
- [16] R. Peng, C. Du, A. Hu et al., "Fabrication of core-shell type poly(NIPAm)-encapsulated citral and its application on bamboo as an anti-molding coating," *RSC Advances*, vol. 11, no. 58, pp. 36884–36894, 2021.
- [17] M. Maswal and A. A. Dar, "Formulation challenges in encapsulation and delivery of citral for improved food quality," *Food Hydrocolloids*, vol. 37, pp. 182–195, 2014.
- [18] Z. Aytac, A. Celebioglu, Z. I. Yildiz, and T. Uyar, "Efficient encapsulation of citral in fast-dissolving polymer-free electrospun nanofibers of cyclodextrin inclusion complexes: high thermal stability, longer shelf-life, and enhanced water solubility of citral," *Nanomaterials*, vol. 8, no. 10, Article ID 793, 2018.
- [19] C. Barreiro, H. Albano, J. Silva, and P. Teixeira, "Role of flies as vectors of foodborne pathogens in rural areas," *International Scholarly Research Notices*, vol. 2013, Article ID 718780, 7 pages, 2013.
- [20] L. A. Ramírez-Camejo, G. Maldonado-Morales, and P. Bayman, "Differential microbial diversity in *Drosophila melanogaster*: are fruit flies potential vectors of opportunistic pathogens?" *International Journal of Microbiology*, vol. 2017, Article ID 8526385, 6 pages, 2017.
- [21] E. P. Black, G. J. Hinrichs, S. J. Barcay, and D. B. Gardner, "Fruit flies as potential vectors of foodborne illness," *Journal of Food Protection*, vol. 81, no. 3, pp. 509–514, 2018.
- [22] A. J. Drummond and R. D. Waigh, "The development of microbiological methods for phytochemical screening," *Recent Research Developments in Phytochemistry*, vol. 4, pp. 143–152, 2000.
- [23] P. D. Shaw, G. Ping, S. L. Daly et al., "Detecting and characterizing *N*-acyl-homoserine lactone signal molecules by thin-layer chromatography," *Proceedings of the National Academy of Sciences*, vol. 94, no. 12, pp. 6034–6041, 1997.
- [24] A. Anitha, V. G. Deepagan, V. V. Divya Rani, D. Menon, S. V. Nair, and R. Jayakumar, "Preparation, characterization, *in vitro* drug release and biological studies of curcumin loaded dextran sulphate-chitosan nanoparticles," *Carbohydrate Polymers*, vol. 84, no. 3, pp. 1158–1164, 2011.
- [25] P.-J. Lu, W.-E. Fu, S.-C. Huang et al., "Methodology for sample preparation and size measurement of commercial ZnO nanoparticles," *Journal of Food and Drug Analysis*, vol. 26, no. 2, pp. 628–636, 2018.
- [26] R. Tantra, P. Schulze, and P. Quincey, "Effect of nanoparticle concentration on zeta-potential measurement results and reproducibility," *Particuology*, vol. 8, no. 3, pp. 279–285, 2010.
- [27] K. Sharma, P. Nirbhavane, S. Chhibber, and K. Harjai, "Sustained release of zingerone from polymeric nanoparticles: an anti-virulence strategy against *Pseudomonas aeruginosa*," *Journal of Bioactive and Compatible Polymers*, vol. 35, no. 6, pp. 538–553, 2020.
- [28] S. Jadhav, R. Shah, M. Bhave, and E. A. Palombo, "Inhibitory activity of yarrow essential oil on *Listeria* planktonic cells and biofilms," *Food Control*, vol. 29, no. 1, pp. 125–130, 2013.
- [29] S. Stepanović, D. Vuković, V. Hola et al., "Quantification of biofilm in microtiter plates: overview of testing conditions and practical recommendations for assessment of biofilm production by staphylococci," *Journal of Pathology, Microbiology and Immunology - the APMIS Journal*, vol. 115, no. 8, pp. 891–899, 2007.
- [30] A. J. Hayes and B. Markovic, "Toxicity of Australian essential oil *Backhousia citriodora* (lemon myrtle). Part 1. Antimicrobial activity and *in vitro* cytotoxicity," *Food and Chemical Toxicology*, vol. 40, no. 4, pp. 535–543, 2002.
- [31] J. Aiensaard, S. Aiumlamai, C. Aromdee, S. Taweechaisupapong, and W. Khunkitti, "The effect of lemongrass oil and its major components on clinical isolate mastitis pathogens and their mechanisms of action on *Staphylococcus aureus* DMST 4745," *Research in Veterinary Science*, vol. 91, no. 3, pp. e31–e37, 2011.
- [32] A. O. Gill, P. Delaquis, P. Russo, and R. A. Holley, "Evaluation of antilisterial action of cilantro oil on vacuum packed ham," *International Journal of Food Microbiology*, vol. 73, no. 1, pp. 83–92, 2002.
- [33] D. Chenthamara, S. Subramaniam, S. G. Ramakrishnan et al., "Therapeutic efficacy of nanoparticles and routes of administration," *Biomaterials Research*, vol. 23, no. 1, Article ID 20, 2019.
- [34] M. Soltanzadeh, S. H. Peighambaroust, B. Ghanbarzadeh, M. Mohammadi, and J. M. Lorenzo, "Chitosan nanoparticles encapsulating lemongrass (*Cymbopogon commutatus*) essential oil: physicochemical, structural, antimicrobial and *in-vitro* release properties," *International Journal of Biological Macromolecules*, vol. 192, pp. 1084–1097, 2021.
- [35] N. P. Thuong Nhan, V. T. Thanh, M. H. Cang et al., "Micro-encapsulation of lemongrass (*Cymbopogon citratus*) essential oil via spray drying: effects of feed emulsion parameters," *Processes*, vol. 8, no. 1, Article ID 40, 2020.
- [36] A. Negi and K. K. Kesari, "Chitosan nanoparticle encapsulation of antibacterial essential oils," *Micromachines*, vol. 13, no. 8, Article ID 1265, 2022.
- [37] D. G. Barrera-Ruiz, G. C. Cuestas-Rosas, R. I. Sánchez-Mariñez et al., "Antibacterial activity of essential oils encapsulated in chitosan nanoparticles," *Food Science and Technology*, vol. 40, no. suppl 2, pp. 568–573, 2020.
- [38] A. G. Luque-Alcaraz, M. O. Cortez-Rocha, C. A. Velázquez-Contreras et al., "Enhanced antifungal effect of chitosan/pepper tree (*Schinus molle*) essential oil bionanocomposites on the viability of *Aspergillus parasiticus* spores," *Journal of Nanomaterials*, vol. 2016, Article ID 6060137, 10 pages, 2016.
- [39] M. Hadidi, S. Pouramin, F. Adinepour, S. Haghani, and S. M. Jafari, "Chitosan nanoparticles loaded with clove essential oil: characterization, antioxidant and antibacterial activities," *Carbohydrate Polymers*, vol. 236, Article ID 116075, 2020.